AIAA 80-0713R

Boundary-Layer Hygroscopic Stresses in Angle-Ply Composite Laminates

S. S. Wang* and I. Choi†
University of Illinois at Urbana-Champaign, Urbana, Illinois

Hygroscopically induced stress fields near geometric boundaries of finite-width, angle-ply composite laminates are investigated. The study is formulated on the basis of the theory of anisotropic hygroelasticity. By the introduction of Lehknitskii's complex stress potentials, governing partial differential equations of the sixth order are established for composite laminates subjected to uniformly distributed moisture change. The hygroscopic stress singularity at the edges of a composite laminate is determined by an eigenfunction expansion technique. Distributions of stresses and associated strain energy density in the boundary-layer region are obtained by using a boundary-collocation method. A symmetric angle-ply [45°/−45°/−45°/45°] graphite-epoxy is chosen for illustrative purposes. The solution for the $[\pm 45°]_s$ composite is presented to elucidate the fundamental nature of hygroscopic edge stresses in composite laminates. Of particular interest are the presently introduced hygroscopic boundary-layer stress intensity factors and their implications.

Introduction

MOISTURE diffusion in anisotropic heterogeneous composites has been shown to result in significant changes in their physical properties[1-3] and dimensional stability,[4,5] which are critically important in the design and analyses of composite materials and structures. These phenomena are most significant in polymer-based, fiber-reinforced composite materials during service in severe hygroscopic environments. The change of physical properties may include alteration of the glass transition temperature of polymeric resin, reduction of mechanical strength, and degradation of fracture and fatigue resistance of the composites. The dimensional change results from swelling or dilatation due to moisture absorption by the composites. Dilatations induced by moisture intake in a fiber-reinforced lamina are anisotropic in general; swelling is restrained in the fiber direction, but develops very appreciably in the transverse direction. In commonly used multilayer composites with angle-ply configurations, these phenomena become more critical than in a unidirectional case, because lateral constraints between adjacent plies lead to the establishment of significant residual stresses.[6,7] The hygroscopically induced stresses and deformations coupled with the moisture degradation of material properties may cause crazing, cracking, and structural failure of the composites. These problems are aggravated further in finite-width composite laminates subjected to severe humidity conditions, because high stress concentrations usually occur along laminate edges due to geometric and material discontinuities.

The response of a composite laminate near its geometric boundaries subjected to hygroscopic and other environmental loading has attracted much attention to date because unanticipated failure of composite structures is frequently initiated at the edges. The hygroscopic stress field in the vicinity of laminate boundaries, i.e., the so-called hygroscopic boundary-layer stresses, which might be primarily responsible for strength degradation and failure of composites, has been investigated by several researchers using different approximate methods.[8,9] The approximate solutions for the boundary-layer effects have revealed unusual features of the problem. Interlamina stresses have been found to be very high and inherently three-dimensional in nature[8,9] near a traction-free boundary of a composite laminate subjected to a uniform change of moisture concentration. The high hygroscopic stresses are also reported[8,9] to be confined within a localized region of several laminar thicknesses from the edge, and in the boundary-layer region they cannot be assessed accurately with classical lamination theory. The behavior of this highly stressed boundary-layer region is of great importance in controlling the complex failure modes and performance of the composites. Understanding the fundamental nature of hygroscopic boundary-layer stresses is essential to the design, failure analysis, and serviceability of composite structures. In this paper, a study of hygroscopic boundary-layer stress singularity and distributions in angle-ply composite laminates subjected to uniform moisture loading is presented.

Presented as Paper 80-0713 at the AIAA/ASME/ASCE/AHS 21st Structures, Structural Dynamics and Materials Conference, Seattle, Wash., May 12-14, 1980, submitted March 19, 1980; revision received Feb. 16, 1982.

*Associate Professor, Dept. of Theoretical and Applied Mechanics. Member AIAA.

†Research Associate, Dept. of Theoretical and Applied Mechanics.

Governing Partial Differential Equations and Solutions

Consider a composite laminate composed of fiber-reinforced plies subjected to mechanical and hygroscopic loading, as shown in Fig. 1. Denote the constitutive equations of each individual ply by the Duhamel-Neumann form of generalized Hooke's law in contracted notation as

$$\epsilon_i = S_{ij}\sigma_j + \beta_i \Delta m \qquad i,j = 1,2,3,\ldots,6 \tag{1}$$

where the repeated subscript indicates summation; S_{ij} is the compliance tensor; β_i the hygroscopic expansion coefficient; and Δm the change of moisture concentration from a reference state. The engineering strains are denoted by $\epsilon_1 = \epsilon_x$, $\epsilon_2 = \epsilon_y, \ldots, \epsilon_6 = \gamma_{xy}$, and the stresses are defined in an analogous manner in Cartesian coordinates.

Formulation of the problem is based on the theory of anisotropic hygroelasticity, and follows the same procedure given in Ref. 10 with the thermal terms $\alpha_i \Delta T$ being replaced by the present equivalent hygroscopic terms $\beta_i \Delta m$. All the details in the formulation are given in Ref. 10 and not repeated in this paper. Only a brief description of the governing differential equations and associated boundary and end conditions for the problem is given here.

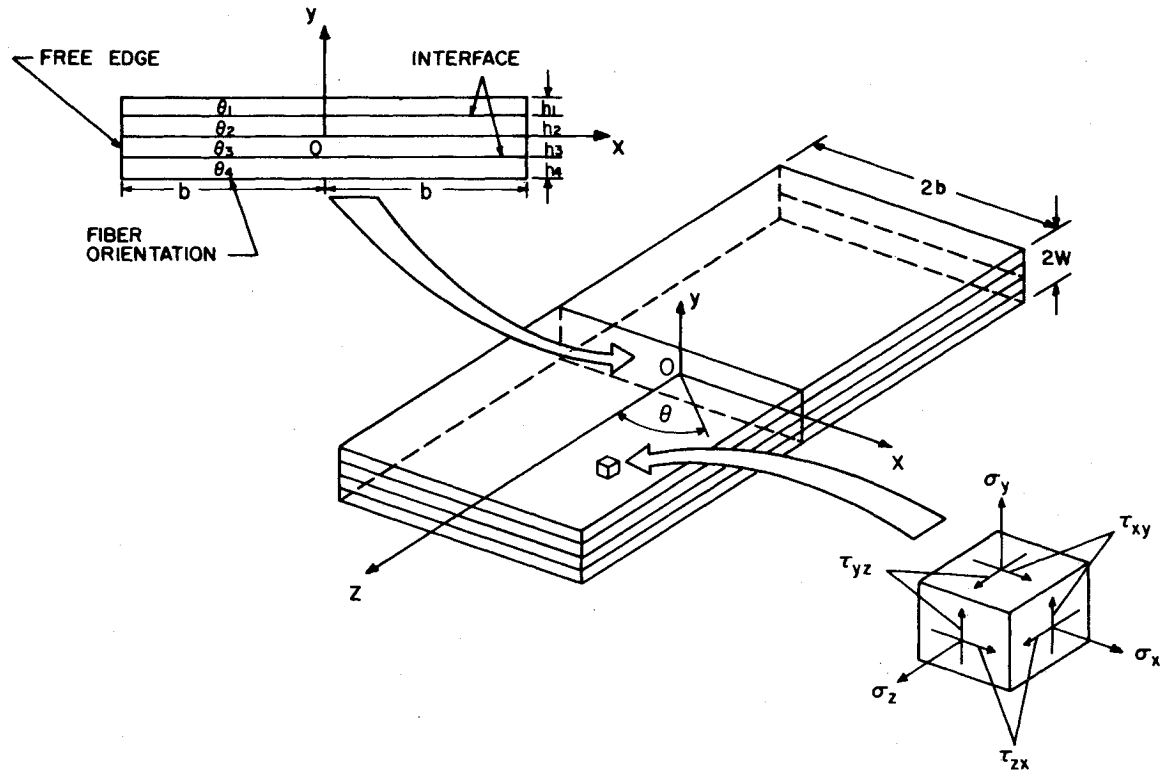

Fig. 1 Coordinates and geometry of an angle-ply $[\theta_1/\theta_2/\theta_3/\theta_4]$ composite laminate.

Governing Partial-Differential Equations and Associated Boundary and End Conditions

For simplicity, but without loss of generality, we introduce the following geometric and environmental conditions for the present hygroscopic boundary-layer study:

1) The composite laminate has a finite width $2b$ (Fig. 1) and is sufficiently long along the z axis that end effects can be neglected by virtue of Saint Venant's principle.

2) The ply interface is a straight line meeting traction free edges of the laminate at $x = \pm b$ at a right angle (Fig. 1).

3) The moisture concentration Δm is constant and uniformly distributed throughout the composite.

4) No mechanical loading is applied.

Using the constitutive equations, the strain-displacement relationships, the equations of equilibrium, and the Lehknitskii complex stress potentials $F(x,y)$ and $\Psi(x,y)$,[11] and following the same procedure given in Ref. 10, we obtain the following pair of coupled governing partial differential equations:

$$L_3F + L_2\Psi = -2A_4 + A_1S_{34} - A_2S_{35} \tag{2a}$$

$$L_4F + L_3\Psi = 0 \tag{2b}$$

where A_1, A_2, and A_4 are constants related to bending and twisting of the laminate, and L_2, L_3, and L_4 are linear differential operators of the second, third, and fourth orders defined by

$$L_2 = \tilde{S}_{44}\frac{\partial^2}{\partial x^2} - 2\tilde{S}_{45}\frac{\partial^2}{\partial x\partial y} + \tilde{S}_{55}\frac{\partial^2}{\partial y^2} \tag{2c}$$

$$L_3 = -\tilde{S}_{24}\frac{\partial^3}{\partial x^3} + (\tilde{S}_{25} + \tilde{S}_{46})\frac{\partial^3}{\partial x^2\partial y} - (\tilde{S}_{14} + \tilde{S}_{56})\frac{\partial^3}{\partial x\partial y^2} + \tilde{S}_{15}\frac{\partial^3}{\partial y^3} \tag{2d}$$

$$L_4 = \tilde{S}_{22}\frac{\partial^4}{\partial x^4} - 2\tilde{S}_{26}\frac{\partial^4}{\partial x^3\partial y} + (2\tilde{S}_{12} + \tilde{S}_{66})\frac{\partial^4}{\partial x^2\partial y^2} - 2\tilde{S}_{16}\frac{\partial^4}{\partial x\partial y^3} + \tilde{S}_{11}\frac{\partial^4}{\partial y^4} \tag{2e}$$

in which $\tilde{S}_{ij}$ are reduced compliance tensors defined as

$$\tilde{S}_{ij} = S_{ij} - S_{3i}S_{j3}/S_{33} \qquad i,j = 1,2,4,5,6 \tag{2f}$$

Boundary conditions associated with traction-free lateral surfaces ∂B‡ of a laminate cross section B shown in Fig. 2 are

$$\sigma_{ij}n_j = 0 \tag{3a}$$

where n_j are directional cosines of the outward unit normal to ∂B. The composite is free to deform without any imposed boundary and end constraints. The hygrothermally induced stresses are clearly self-equilibrating on any laminate cross section. Thus for a cross section of the laminate, the statically equivalent loading can be expressed by

$$\iint_B \sigma_z dxdy = \iint_B \sigma_z x dxdy = \iint_B \sigma_z y dxdy = 0 \tag{3b}$$

$$\iint_B (\tau_{yz}x - \tau_{xz}y)dxdy = 0 \tag{3c}$$

Homogeneous and Particular Solutions for Hygroscopic Boundary-Layer Stresses

The governing equations (2a) and (2b) are coupled, linear partial-differential equations with coefficients involving anisotropic elastic mechanical and hygroscopic constants of each individual lamina. With the aid of the associated boundary conditions previously mentioned, the general solution, consisting of a homogeneous part and a particular

‡∂B is the boundary of domain B.

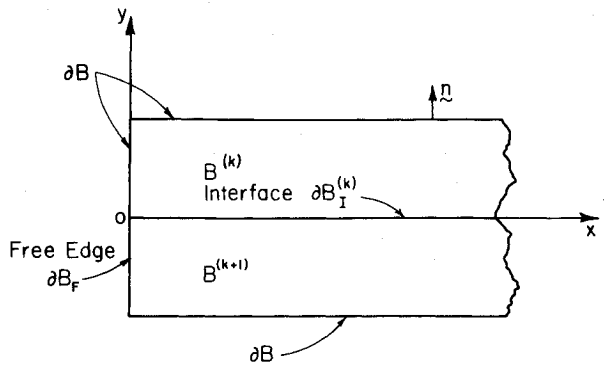

Fig. 2 Free-edge geometry and the interface between kth and $(k+1)$th plies.

solution, can be constructed for a composite laminate with a given geometry, ply configuration, and hygroscopic environmental condition. The detailed method of analysis and the solution procedure for the coupled partial-differential equations have been discussed in related papers.[10,13] Only the final forms of the homogeneous and particular solutions are given here for completeness.

Introducing a proper form for the Lehknitskii complex stress functions and using an eigenfunction expansion method as described in Ref. 10, one can establish the homogeneous solution for the problem as

$$\sigma_x^{(h)} = \sum_{k=1}^{3} (C_k \mu_k^2 Z_k^\lambda + C_{k+3} \bar{\mu}_k^2 \bar{Z}_k^\lambda) \tag{4a}$$

$$\sigma_y^{(h)} = \sum_{k=1}^{3} (C_k Z_k^\lambda + C_{k+3} \bar{Z}_k^\lambda) \tag{4b}$$

$$\tau_{yz}^{(h)} = -\sum_{k=1}^{3} (C_k \eta_k Z_k^\lambda + C_{k+3} \bar{\eta}_k \bar{Z}_k^\lambda) \tag{4c}$$

$$\tau_{xz}^{(h)} = \sum_{k=1}^{3} (C_k \eta_k \mu_k Z_k^\lambda + C_{k+3} \bar{\eta}_k \bar{\mu}_k \bar{Z}_k^\lambda) \tag{4d}$$

$$\tau_{xy}^{(h)} = -\sum_{k=1}^{3} (C_k \mu_k Z_k^\lambda + C_{k+3} \bar{\mu}_k \bar{Z}_k^\lambda) \tag{4e}$$

$$u^{(h)} = \sum_{k=1}^{3} (C_k p_k Z_k^{\lambda+1} + C_{k+3} \bar{p}_k \bar{Z}_k^{\lambda+1}) / (\lambda+1) \tag{5a}$$

$$v^{(h)} = \sum_{k=1}^{3} (C_k q_k Z_k^{\lambda+1} + C_{k+3} \bar{q}_k \bar{Z}_k^{\lambda+1}) / (\lambda+1) \tag{5b}$$

$$w^{(h)} = \sum_{k=1}^{3} (C_k t_k Z_k^{\lambda+1} + C_{k+3} \bar{t}_k \bar{Z}_k^{\lambda+1}) / (\lambda+1) \tag{5c}$$

where $Z_k = x + \mu_k y$ with μ_k being roots of the algebraic characteristic equation given in Ref. 10; λ is the eigenvalue related to the order of boundary-layer stress and deformation fields; C_k are complex constants to be determined; and p_k, q_k, and t_k are known constants given in Ref. 10. The homogeneous solutions for stresses and displacements are required to satisfy traction-free boundary conditions and interface continuity conditions, leading to a standard eigenvalue problem. The exponent λ in Eqs. (4) and (5) can be determined by solving a transcendental characteristic equation resulting from the condition for a nontrivial solution.[12,13]

The particular solutions for the governing partial-differential equations with the associated boundary and end conditions may be sought for in the form of polynomials, and are found to have the following forms[10,13]:

$$\sigma_x^{(p)} = 2a_3 x + 6a_4 y + 2a_7 \tag{6a}$$

$$\sigma_y^{(p)} = 6a_1 x + 2a_2 y + 2a_5 \tag{6b}$$

$$\tau_{yz}^{(p)} = -2a_8 x - a_9 y - a_{11} \tag{6c}$$

$$\tau_{xz}^{(p)} = a_9 x + 2a_{10} y + a_{12} \tag{6d}$$

$$\tau_{xy}^{(p)} = -2a_2 x - 2a_3 y - a_6 \tag{6e}$$

$$u^{(p)} = -\tfrac{1}{2} A_1 S_{33} z^2 - A_4 yz + U^{(p)}(x,y) + \omega_2 z - \omega_3 y + u_0 \tag{7a}$$

$$v^{(p)} = -\tfrac{1}{2} A_2 S_{33} z^2 + A_4 xz + V^{(p)}(x,y) + \omega_3 x - \omega_1 z + v_0 \tag{7b}$$

$$w^{(p)} = (A_1 x + A_2 y + A_3) S_{33} z + W^{(p)}(x,y) + \omega_1 y - \omega_2 x + w_0 \tag{7c}$$

where a_i $(i=1,2,\ldots,12)$ are arbitrary constants to be determined later; $U^{(p)}$, $V^{(p)}$, and $W^{(p)}$ are functions involving material constants, S_{ij} and β_i, and x and y only with their forms given in Ref. 10. The particular solutions are required to satisfy the governing differential equations and remote boundary conditions. With the given end conditions imposed by Eqs. (3b) and (3c), these unknown constants can be easily solved.[10]

Complete Solutions

The complete solution for the boundary-layer hygroscopic stress problem can be written as

$$\sigma_i = \sigma_i^{(h)} + \sigma_i^{(p)} \qquad i=1,2,4,5,6 \tag{8a}$$

$$u_j = u_j^{(h)} + u_j^{(p)} \qquad j=1,2,3 \tag{8b}$$

The solution for the stresses in Eq. (8a) satisfies identically the boundary conditions along free-edge surfaces. Along ∂B_s $(=\partial B - \partial B_f)$, residual stresses appear due to the particular solution established in the previous section. The mismatched stresses on ∂B_s can be counterbalanced by using the homogeneous solution and the following relationship:

$$\sigma_{ij}^{(h)} n_j + \sigma_{ij}^{(p)} n_j = 0 \tag{9}$$

Without the orthogonality conditions among the eigenfunctions, Eq. (9) can be satisfied numerically by truncating the eigenfunction series through a boundary-collocation procedure.[13] Thus by matching Eq. (9) with the aid of Eq. (3) one can determine all the unknowns explicitly. The expressions for σ_z can be obtained as

$$\sigma_z^{(h)} = -S_{3j} \sigma_j^{(h)} / S_{33} \qquad j=1,2,4,5,6 \tag{10a}$$

$$\sigma_z^{(p)} = A_1 x + A_2 y + A_3 - (S_{3j} \sigma_j^{(p)} + \beta_3 \Delta m) / S_{33} \tag{10b}$$

Complete expressions for the displacement field can be determined explicitly in a similar manner.

Numerical Example and Discussion

In this section the fundamental behavior of hygroscopic boundary-layer stresses is studied in detail. The specific objective is to determine the exact hygroscopic stress singularity, stress distributions, and the boundary-layer thickness near the edges of a composite laminate. For the composite with a specific laminate configuration and fiber orientations, the general solution outlined in the previous section can be programmed in a numerical scheme suitable for computation. Additional geometric and material symmetry

conditions are introduced to simplify the formulation further. The particular solution corresponding to the loading and boundary conditions of the problem is determined by using a boundary-collocation method.[13]

For illustrative purposes, a symmetric, angle-ply graphite-epoxy composite laminate with a [45°/−45°/−45°/45°] fiber orientation is chosen in this study. The width-to-thickness ratio of the laminate, $2b/2W$, is 4, and each individual ply has a uniform thickness $h_i (i=1,2,3,4)$ with $h_i = h = \frac{1}{2}W$ (Fig. 1). For simplicity without loss of generality, only hygroscopic loading of unit moisture concentration ($\Delta m = 1\%$) distributed uniformly throughout the laminate is considered. The following ply properties§ typical of high-modulus unidirectional graphite-epoxy composite are used in computation: $E_L = 137.9$ GPa (20.0×10^6 psi), $E_T = 14.48$ GPa (2.1×10^6 psi), $G_{LT} = G_{Lz} = G_{Tz} = 5.86$ GPa (0.85×10^6 psi), $\nu_{LT} = \nu_{Lz} = \nu_{Tz} = 0.21$, $\beta_L = 0.0$, $\beta_T = \beta_z = 6.67\times10^{-3}$/wt.%, where subscripts L, T, and z refer to the longitudinal, transverse, and thickness directions of the individual ply, respectively.

The accuracy and convergence study of the solutions has been conducted and is extremely lengthy. The results have been documented in Ref. 13 in detail and, therefore, are not repeated here. The effects of the number of terms used in the eigenfunction series and the number of stations used in the boundary collocation have also been reported in Ref. 13. In the present numerical calculation, 63 terms in the eigenfunction series and 74 collocation points along the boundaries are used. Based on the convergence study of Ref. 13, the results given in this paper should be within a 2% difference from the converged solutions. In what follows, a detailed solution for the $[\pm45°]_s$ graphite-epoxy laminate subjected to the aforementioned unit hygroscopic loading condition is presented to illustrate the fundamental nature of the hygroscopic boundary-layer effects.

Boundary-Layer Hygroscopic Stress Distribution Along Ply Interface

Distributions of in-plane and interlaminar stress components along the 45°/−45° ply interface are given in Fig. 3. The vertical axis represents the stresses at the interface in MPa (ksi) per 1% wt. change of moisture concentration in the laminate, and the horizontal axis denotes the distance away from the center of the panel. The in-plane stresses σ_x, σ_z, and τ_{xz} in the region away from the laminate boundary are found to be relatively constant and to recover to more or less what classical lamination theory (CLT) predicts. Based on classical lamination theory, the only stress induced by a unit weight change of moisture concentration in the $[\pm45°]_s$ graphite-epoxy is the constant in-plane shear stress $\tau^{\circ}_{xz} = 84.12$ MPa (12.2 ksi). The in-plane normal stress σ_z in the far field is small and remains less than 6.895 MPa (1 ksi), which is distinct from what is predicted with CLT, i.e., $\sigma^{\circ}_z = 0$. As the edge is approached, the differences become very appreciable due to the presence of the boundary-layer stress singularity which is not included in the laminated plate theory. Within the boundary-layer region, the in-plane stresses are intensified significantly, and there exist rapidly increasing interlaminar stresses, τ_{yz} and σ_y, which classical lamination theory fails to predict. In fact, the interlaminar stresses become much larger than the in-plane stress components as the edge of the laminate is infinitesimally approached; thus, the hygroscopic deformation and failure might be dominated by the interlaminar stresses.

§Values of the shear modulus G_{Tz} and Poisson's ratio ν_{Tz} employed here, which were also used in previous studies,[8-10,12-15] are recognized to be hypothetical and are only for illustration of the general nature of the present problem. More appropriate values for the properties are $\nu_{Tz} \simeq 1.5\,\nu_{LT} = 0.32$ and $G_{Tz} \simeq 0.6\,G_{LT} = 3.52$ GPa (0.51×10^6 psi). The results obtained by using these more appropriate elastic constants differ from those given in this paper by approximately 10%.[14]

Hygroscopic Stress Singularity

It is now clear that the stress and strain fields within the boundary-layer region are completely governed by the singular terms in the present hygroelasticity solutions. Theoretically, the hygroscopically induced stresses determined from the solution are unbounded at the intersection of the ply interface and the edge of the laminate. Thus, the near-field stresses may be expressed in a general form as

$$\sigma_i = \sum_{k=1}^{3} \left(D_{ik} Z_k^{\lambda_l} + D_{i(k+3)} \bar{Z}_k^{\lambda_l}\right) + 0\ (\text{higher-order, nonsingular terms}) \quad (i=1,2,3,\ldots,6) \tag{11}$$

where Z and $\bar{Z}$ have their origin located at the intersection of the 45°/−45° ply interface and the edge of the laminate (Fig. 2); λ_l is the order of the boundary-layer stress singularity which is the smallest eigenvalue with

$$0 > Re(\lambda_l) > -1 \tag{12}$$

among all the λ_m determined from the transcendental equation[12,13] in solving for the homogeneous solution of the governing partial-differential equations. The order of the boundary-layer stress singularity depends only upon lamina constitutive properties and fiber orientations of the adjacent plies. Numerical results of the first six nonzero eigenvalues λ_m for the [45°/−45°/−45°/45°] graphite-epoxy laminate are

$$\lambda_l = -0.02558, \qquad \lambda_{2,3} = 0.88147 \pm 0.23400i$$

$$\lambda_4 = 1.0, \qquad \lambda_{5,6} = 1.51153 \pm 0.79282i$$

Note that λ_l corresponds to the order of the boundary-layer stress singularity and that zero and integers n ($=1,2,3,\ldots$) are always eigenvalues for the problem. In this composite system, λ_l has a value that is rather weak compared with other typical singular stress problems such as an elastic crack problem.

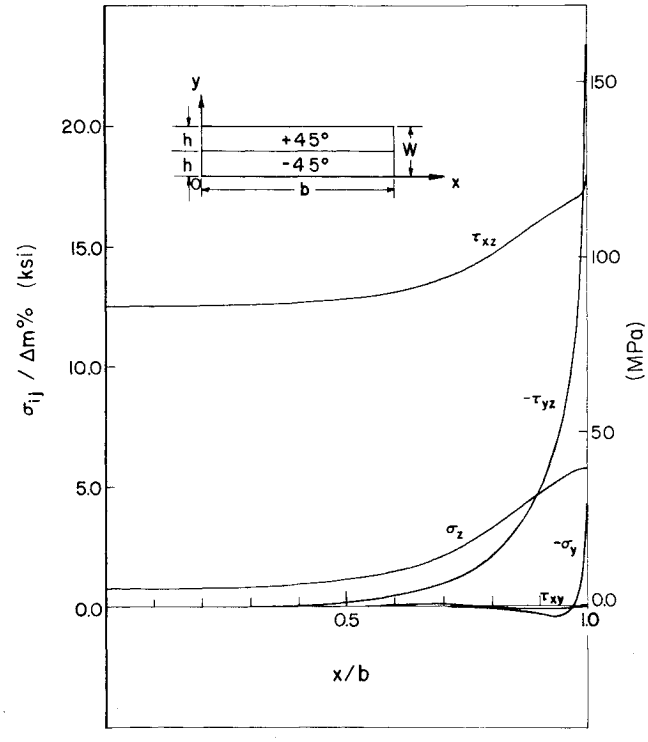

Fig. 3 In-plane and interlaminar hygroscopic stresses along ply interface in $[\pm45°]_s$ graphite-epoxy composite.

Hygroscopic Boundary-Layer Stress Intensity Factors

For a composite laminate with given fiber orientations, the coefficients in the singular terms of Eq. (11) characterize amplitudes of the hygroscopic stresses and strains in the boundary-layer region. Because the boundary-layer stresses are most crucial along the interface, i.e., the x axis, and become singular at the interface/edge intersection, it is possible to define the amplitudes of the singular, interface boundary-layer stresses by

$$K_i = \lim_{x\to 0} x^{-\lambda_1}\sigma_i \qquad i=1,2,3,\ldots,6 \tag{13}$$

The K_i are dependent upon geometric variables of the composite (e.g., ply thickness, number of layers), laminate parameters (e.g., fiber orientation, stacking sequence), and mechanical and hygroscopic loading conditions. The fundamental structure of the hygroscopic boundary-layer stress solution shown in Eqs. (11) and (13) resembles that of an elastic crack problem (except that λ_1 has a vlaue of -0.5 in the crack-tip stress field). Also, the nature of K_i is similar to the so-called crack-tip stress intensity factors in linear elastic fracture mechanics. Thus in this context it may be appropriate to denote K_i as "boundary-layer hygroscopic stress intensity factors" or "free-edge hygroscopic stress intensity factors" for the composite laminate. Values of K_i for the [45°/−45°/−45°/45°] graphite-epoxy composite with all laminae being of equal thicknesses under unit hygroscopic loading are determined as follows:

$$K_1 = 4.6835E-2 \quad K_2 = -6.1587E-1 \quad K_3 = -2.4132E-3$$

$$K_4 = -1.3440E\ 0 \quad K_5 = 1.1803E-1 \quad K_6 = 0$$

where K_i carry the unit of MPa-m$^{-\lambda_1}$.

The K_i associated with the interlaminar stresses are found, in general, to be significantly larger than those associated with the in-plane stress components. The dominance of the interlaminar stresses σ_y and τ_{yz} in the boundary-layer region shown in Fig. 3 is clearly illustrated by the large values of K_2 and K_4, which are, in fact, one or two orders of magnitude higher than the K_i associated with σ_x, σ_z, and τ_{xz}. The high negative value of K_2 indicates that a large compressive interlaminar normal stress σ_y is developed near the edge. Note that K_6 is found to vanish for all angle-ply $[\pm\theta]_s$ composite laminates,[15] due to the symmetry of ply orientations and the traction-free edge condition.

Hygroscopic Stress Distributions Through Laminate Thickness

The unique features of the hygroscopic boundary-layer effects are further illustrated by through-the-thickness distributions of the moisture-induced stresses in the composite. Distributions of the in-plane stress σ_z along the y direction are depicted in Fig. 4 at several distances x/b away from the center of the panel. The σ_z is found to be small in tension in the far field, for example, $x/b=0.5$. Near the edge, the stress changes appreciably into compression in the most part of the laminate cross section except for the region closest to the 45°/−45° ply interface where the high tensile stress develops rapidly. Very near the edge, say $x/b=0.999$, the

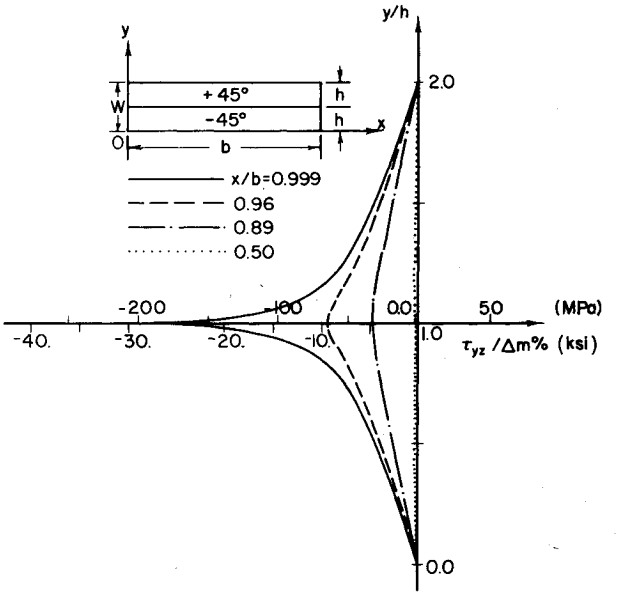

Fig. 5 Through-laminate-thickness distributions of boundary-layer hygroscopic stress τ_{yz} at various x/b in [45°/−45°/−45°/45°] graphite-epoxy composite laminate.

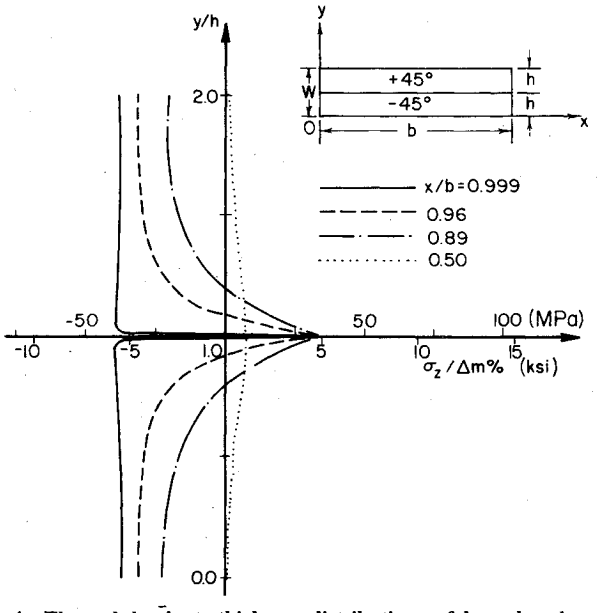

Fig. 4 Through-laminate-thickness distributions of boundary-layer hygroscopic stress σ_z at various x/b in [45°/−45°/−45°/45°] graphite-epoxy composite laminate.

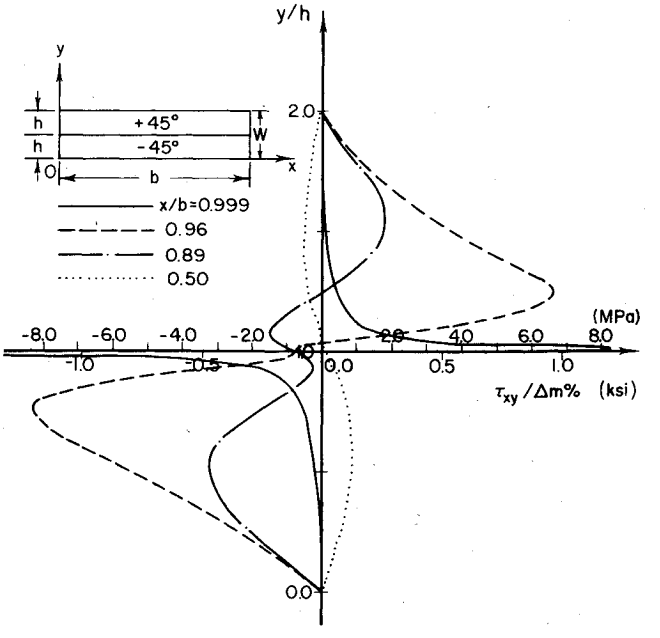

Fig. 6 Through-laminate-thickness distributions of boundary-layer hygroscopic stress τ_{xy} at various x/b in [45°/−45°/−45°/45°] graphite-epoxy composite laminate.

compressive σ_z remains approximately constant through the thickness direction except in the very local region near the interface, $y=h$. Through-laminate-thickness distributions of the most dominant interlaminar shear stress τ_{yz} are given in Fig. 5. The stress gradient of τ_{yz} in the y direction varies drastically as the edge of the laminate is approached. At any given distance x/b, the interlaminar stress changes approximately symmetrically in the outer and inner plies, due to the $\pm\theta$ fiber orientations. In the boundary-layer region, the value of the interlaminar shear stress near the interface of 45° and −45° plies is shown to increase very significantly, usually by an order of magnitude, as one moves toward the edge by a small amount of x/b, say from $x/b=0.89$ to 0.999.

Information on through-thickness distributions of the other hygroscopic interlaminar shear stress τ_{xy} is given in Fig. 6. In the near field, τ_{xy} changes very significantly with the thickness coordinate and alters its sign across the ply interface. The sign change across the interface is mainly caused by the orthogonality of fiber orientations between the +45° and −45° plies. The interlaminar shear stress component reaches its maximum value at a very small distance y away from the interface along $x/b=0.999$ and vanishes at the boundary of the laminate as evidenced by the zero value of K_6. Distributions of the hygroscopic interlaminar normal stress σ_y at several distances near the boundary of the laminate are shown in Fig. 7. At a given distance x/b, σ_y is very small at any position y away from and at the ply interface in general. The situation changes significantly when the edge is approached. For example, at $x/b=0.999$, the interlaminar normal stress has a very significant value in compression near the interface. At $x\pm b$ and $y=h$, σ_y becomes unbounded due to the presence of the boundary-layer stress singularity.

Hygroscopic Boundary-Layer Width

The rapid increase of hygroscopic stress has been observed to be restricted within a very localized region near the edge of the laminate—the so-called "hygroscopic boundary-layer width." The hygroscopic stresses developed in the boundary-layer region are inherently three-dimensional in nature and cannot be determined by classical lamination theory. The singular nature and the extent of perturbation of the boundary hygroscopic stresses are considered to be of vital importance in controlling initiation of interlaminar fracture (or delamination) and strength degradation. The extent of perturbation of the hygroscopic stress field can be characterized by the boundary-layer width (or thickness), B. Pipes et al.[16] defined the boundary-layer thickness as the distance from the edge, at which interlaminar stress τ_{yz} is about 3% of the value calculated at the intersection of the ply interface and the edge of the laminate. The validity of this definition is somewhat questionable because the interlaminar stresses are singular at the free edge. In this study an alternative definition of the boundary-layer width is proposed on the basis of the strain energy density distribution in the composite laminate.

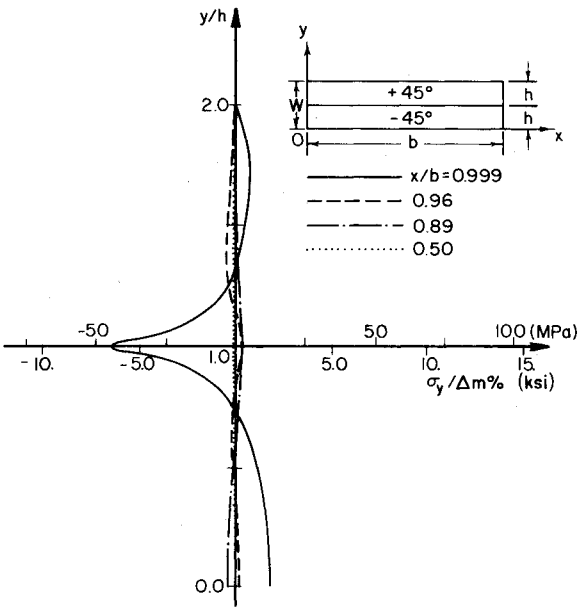

Fig. 7 Through-laminate-thickness distributions of boundary-layer hygroscopic stress σ_y at various x/b in [45°/−45°/−45°/45°] graphite-epoxy composite laminate.

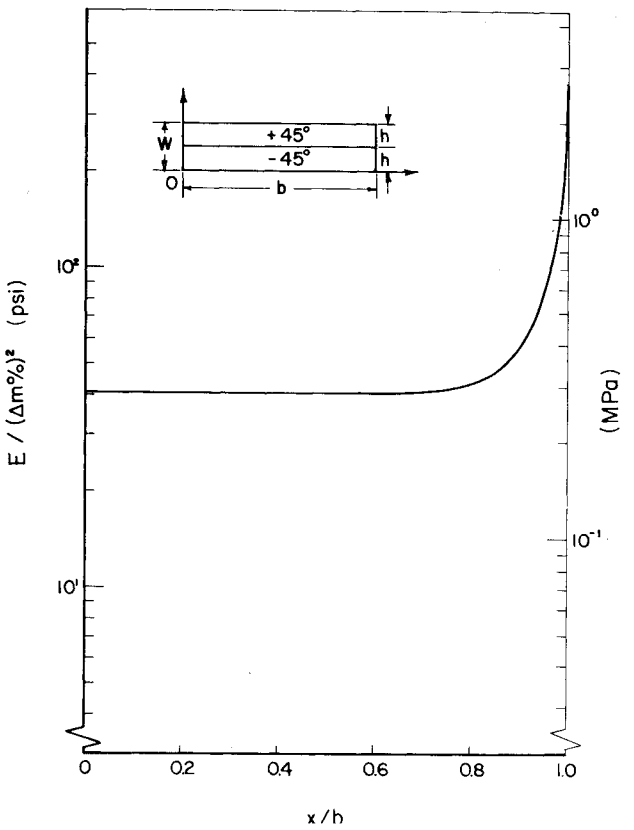

Fig. 8 Strain energy density distribution along the interface $y=h^+$ of [45°/−45°/−45°/45°] graphite-epoxy composite laminate subjected to uniform hygroscopic loading.

The strain energy density distribution $E(x,y)$ along the ply interface in the $[\pm 45°]_s$ graphite-epoxy laminate is shown in Fig. 8. The strain energy density remains relatively constant in the far field where classical lamination theory holds and increases drastically by an order of magnitude as the edge is approached. In this paper, the boundary-layer width B in the composite laminate is defined as the distance away from the edge, where the strain energy density along the interface is 3% higher than the nominal value E_0 obtained in the far field. In general, $E(B,h^+)$ differs slightly from $E(B,h^-)$ due to the discontinuous in-plane stress components at $y=h^+$ and h^-; thus an average value of B is designated as the width of the boundary-layer region. Based on this definition, the B/W for the graphite-epoxy laminate has been found to have a value of approximately 1.1. The [45°/−45°/−45°/45°] graphite-expoxy is noted to have the largest value of B/W as compared with those of other fiber orientations $[\pm\theta]_s$. As θ changes toward either direction, B/W decreases rapidly.[15]

Summary and Conclusions

Boundary-layer hygroscopic stresses in angle-ply composite laminates are studied. The problem formulation is based on the theory of anisotropic hygroelasticity with the aid of Lehknitskii's stress potentials. Solutions based on an eigenfunction expansion method and a boundary-collocation

technique are obtained. The results for a symmetric [45°/−45°/−45°/45°] graphite-epoxy laminate are presented to illustrate the fundamental nature of hygroscopic boundary-layer effects in angle-ply composite laminates. The boundary-layer hygroscopic stress singularity and distributions are determined in detail. Based on the solutions obtained, the following conclusions can be reached:

1) Hygroscopic stresses in the boundary-layer region of an angle-ply composite laminate are inherently three-dimensional in nature. They cannot be calculated by classical lamination theory but can be determined explicitly by the current approach.

2) The hygroscopic stress field in the boundary-layer region of a composite laminate is inherently singular. Using the eigenfunction expansion method, one can determine exactly the order of hygroscopic boundary-layer stress singularity by solving the transcendental characteristic equation from the homogeneous solution for the problem. The boundary-layer stress singularity is found to be rather weak in general and depends only on anisotropic elastic properties and fiber orientations of adjacent plies in the composite laminate.

3) The hygroscopic edge-stress field in a given composite laminate can be characterized by the presently introduced "boundary-layer hygroscopic stress intensity factors" or "free-edge hygroscopic stress intensity factors." The K_i are functions of anisotropic elastic properties and hygroscopic constants of laminae, ply orientation, and laminate geometry, and may be used to evaluate strength degradation, initiation of interlaminar fracture (delamination), and transverse cracking in composite laminates.

4) The hygroscopic boundary-layer width, which characterizes the size of the domain where classical lamination theory does not hold, can be defined and determined explicitly by a proper consideration of the strain energy density distribution along the ply interface. The hygroscopic boundary-layer thickness depends on the ply thickness, laminate geometry, stacking sequence, and anisotropic elastic properties and hygroscopic constants of individual plies.

Acknowledgments

The work described in this paper was supported in part by the NASA Lewis Research Center (NASA-LRC), Cleveland, Ohio under Grant NSG 3044. The authors are grateful to Dr. C. C. Chamis of NASA-LRC, Dr. G. P. Sendeckyj of the Air Force Flight Dynamics Laboratory, Prof. A.S.D. Wang of Drexel University, Prof. R. B. Pipes of the University of Delaware, and Prof. H. T. Corten of the University of Illinois at Urbana-Champaign for the valuable discussion and encouragement during the course of this study.

References

[1] Vinson, J. R. and Walker, W., "The Influence of Relative Humidity and Elevated Temperature on Composite Materials and Structures," Tech. Rept. AFOSR-TR-77-0030, Bolling AFB, Washington, D.C., 1976.

[2] DeIasi, T. and Whiteside, J. B., "Effects of Moisture on Epoxy Resin and Composites," *Advanced Composite Materials—Environmental Effects, ASTM STP 658,* edited by J. R. Vinson, ASTM, Philadelphia, Pa., 1978, pp. 2-20.

[3] Crossman, F. W., Mauri, R. E., and Warren, W. J., "Moisture Altered Viscoelastic Response of Graphite-Epoxy Composites," *Advanced Composite Materials—Environmental Effects, ASTM STP 658*, edited by J. R. Vinson, ASTM, Philadelphia, Pa., 1978, pp. 205-220.

[4] Hahn, H. T. and Kim, R. Y., "Swelling of Composite Laminate," *Advanced Composite Materials—Environmental Effects, ASTM STP 658,* edited by J. R. Vinson, ASTM, Philadelphia, Pa., 1978, pp. 98-120.

[5] Cohen, D. and Maron, G., "A Proposal for a Coefficient of Hygroelasticity," *Polymer Engineering and Science*, Vol. 18, No. 13, Oct. 1978, pp. 1001-1005.

[6] Pipes, R. B., Vinson, J. R., and Chou, T. W., "On the Hygrothermal Response of Laminate Composite Systems," *Journal of Composite Materials,* Vol. 10, April 1976, pp. 129-148.

[7] Chamis, C. C., Lark, R. F., and Sinclair, J. H., "Integrated Theory for Predicting the Hygrothermomechanical Response of Advanced Composite Structural Components," *Advanced Composite Materials—Environmental Effects, ASTM STP 658*, edited by J. R. Vinson, ASTM, Philadelphia, Pa., 1978, pp. 160-192.

[8] Farley, G. L. and Herakovich, C. T., "Influence of Two Dimensional Hygrothermal Gradients on Interlaminar Stresses Near Free-Edges," *Advanced Composite Materials—Environmental Effects, ASTM STP 658*, edited by J. R. Vinson, ASTM, Philadelphia, Pa., 1978, pp. 143-159.

[9] Crossman, F. W. and Wang, A.S.D., "Stress Field Induced by Transient Moisture Sorptions in Finite-Width Composite Laminates," *Journal of Composite Materials*, Vol. 12, Jan. 1978, pp. 2-18.

[10] Wang, S. S. and Choi, I., "Boundary-Layer Thermal Stresses in Angle-Ply Composite Laminates," *Modern Developments in Composite Materials and Structures*, edited by J. R. Vinson, ASME, New York, Dec. 1979, pp. 315-342.

[11] Lehknitskii, S. G., *Theory of Elasticity of an Anisotropic Body*, Holden-Day, San Franscisco, Calif., 1963.

[12] Wang, S. S. and Choi, I., "Boundary-Layer Effects in Composite Laminates," AIAA Paper 79-0803, *Proceedings of the 20th Structures, Structural Dynamics and Materials Conference*, St. Louis, Mo., April 1979.

[13] Wang, S. S. and Choi, I., "Boundary-Layer Effects in Composite Laminates: Part I—Free-Edge Stress Singularity; Part II—Free-Edge Stress Solutions and Basic Characteristics," *Journal of Applied Mechanics, Transactions of ASME*, Vol. 49, No. 3, 1982, pp. 541-560.

[14] Wang, S. S., unpublished data, University of Illinois, Urbana, Ill., 1981.

[15] Wang, S. S. and Choi, I., "Influence of Fiber Orientation and Ply Thickness on Hygroscopic Boundary-Layer Stresses in Angle-Ply Composite Laminates," *Journal of Composite Materials*, Vol. 16, May 1982, pp. 244-258.

[16] Pipes, R. B. and Pagano, N. J., "Interlaminar Stresses in Composite Laminates Under Uniform Axial Extension," *Journal of Composite Materials*, Vol. 4, No. 3, Oct. 1970, pp. 538-548.